AXIAL CAPACITY OF LIGHTWEIGHT AGGREGATE CONCRETE FILLED CIRCULAR STEEL TUBES COLUMNS SUBJECTED TO ECCENTRIC LOADING

Abdelgadir Elzien Abdelgadir[1]and Mohammed G. Seleman[1]

[1]Department of civil Engineering, Faculty of Engineering, University of Nile Valley,
drsha82@hotmail.com
mohgamars86@gmail.com

مُسْتَخْلَص

هدفت هذه الورقة إلى محاولة دراسة سلوك الاعمدة الفولاذية المجوفة رقيقة الجدار و المملوءة بالخرسانة خفيفة الوزن (LACFT) تحت تأثير حمل لا مركزي. تم إجراء الإختبار على 54 عينة دائرية مع اخذ كلاً من : (1) مسافات لا تمركز مختلفة (10 ، 20 و 35 مم) ، (2) نسبة الفولاذ (11% و13.51%) (3) و نسبة نحافة تراوحت بين (3-14) كمتغيرات رئيسية في هذه التجربة. أظهرت المقارنة بين نتائج الحسابات المتحصل عليها من المدونتين (AISC-LRFD) و (CHN DBJ 13-51-2003) قدرة تحمل منخفضة و في حدود المقبول عدا الأعمدة ذات النحافة ($L/D \geq 14$) فكان تقديرها أكبر قليلاً من تلك التي تم قياسها أثناء التجارب على التوالي، في حين أن النتائج التي حققتها المدونة (CHN CECS 28:90) أظهرت اتفاقاً جيداً مع النتائج التجريبية مع زيادة قليلة في حالة الأعمدة ذات النحافة ($L/D \geq 14$) أيضاً. أوضحت هذه الدراسة أن قدرة تحمل الأعمدة الفولاذية LACFT الخاضعة لتحميل اللامركزي هي قدرة محافظة.

ABSTRACT

This paper presents an experimental study on the behavior of lightweight aggregate concrete-filled steel tubes (LACFT) under eccentric loading. 54 circular specimens with different load eccentricity distances (10, 20 and 35mm); thickness to width ratio (t/D=11.4 and 13.5); and length to width ratio (L/D = 3, 7, and 14) tested to examine the bearing capacity. Significant parameters influencing LACFT column's bearing capacity, failure mechanism and failure mode all studied and analyzed. Comparison between the predicted results by AISC-LRFD and CHN DBJ 13-51-2003 codes showed lower and applicable bearing capacities with slightly overestimated values for L/D≥14 than that measured during the experiments respectively, while the results gained by CHN CECS 28:90 showed a good agreement with the experimental results and slightly overestimated the values for L/D≥ 14 too. This study shows that bearing capacity of LACFT steel columns subjected to eccentric loading is conservative.

***Keywords**:* Lightweight Aggregate Concrete Filled Steel Tube, Eccentricity Ratio, Thickness to Width Ratio, Length to Width Ratio, Ultimate Bearing Capacity, Composite Construction

1 Introduction

The use of concrete filled steel tubular (CFT) columns for the construction of high–rise buildings, bridges, barriers, etc. has become increasingly popular in recent years. These columns have demonstrated higher axial load capacity, better ductility performance, larger energy absorption capacity and lower strength degradation than conventional reinforced concrete and steel hollow section column [1]. The enhancement of structural properties of CFT columns is mainly due to the composite action of steel hollow section and core concrete. The confining effect by steel hollow section causes the core concrete to behave in tri-axial stress state while the core concrete prevents the wall of the steel hollow section from buckling inward [2].

In concrete construction, self-weight represents a very large proportion of the total load on the structure, and there are clearly considerable advantages in reducing the density of concrete. One of the ways to reduce the mass or self-weight of a structure is the use of lightweight aggregate in concrete to get lightweight aggregate concrete (LAC). The benefit of lightweight aggregate in concrete as structural material has been recognized as far back as Roman days. Although there is few published data available on the researches of the LACFT but several authors in their investigations reported that LAC has its obvious advantages of higher strength/weight ratio, lightweight, good ductility, convenience of construction, lower coefficient of thermal expansion, and superior heat and sound insulation characteristic due to air voids in the lightweight aggregate [3], [4], [5]. Lightweight aggregate concrete filled steel tube (LACFT) as a new form of composite structures, under the same conditions, not only has the same strength and durability as the CFT, but also reduces the self-weight of the structure by about 20 %. Nowadays, with the trend towards large span bridges and towering direction of building structures, the LACFT with its distinguished characteristics, will have broad applications prospects. However, structural studies on LACFT are still in the initial step all over the world therefore; more researches are needed. Because of CFT component's advantages of high compression strength and good plastic deformation, often used as a compression member, nevertheless, in the practice of actual engineering the influence of the initial defects, material inhomogeneity, manufacturing deviations and other factors, on the ideal axial compression is very difficult to avoid. At the same time the multistory and high-rise buildings under the act of the vertical load, lateral horizontal wind or seismic forces, will also be bore by the moment, hence the component tends to the state of eccentric compression [6]. Consequently, the study of eccentric compression of LACFT will have important and significance role in the theoretical researches and engineering applications value.

This paper attempts to study the structural performance of thin-walled steel columns filled with LAC as a construction material. Based on eccentricity tests, fifty four specimens with different L/D ratios (3, 7 and 14) were tested. The main parameters varied in the tests are: (1) load eccentricity ratio; (2) thickness to width ratio (t/D); and (3) length to width ratio. The standard load-strain curves of LACFT columns under eccentric loading were summarized and significant parameters affecting LACFT column's bearing capacity, failure mechanism and failure pattern were all studied and analyzed through the comparison with calculated strength of CFT columns using the existing codes such as AISC-LRFD [7], CHN DBJ 13-51-2003 [8] and CHN CECS 28:90 [9].

2 Test Arrangements and Procedure

2.1 Specimens and Material

In this study; LACFTs columns with a diameter (D) of 114 mm and two different wall thicknesses (3 and 3.5 mm) are selected. The mix was prepared using ordinary Portland cement (OPC), fly ash - shale ceramic with Bulk density 814 kg/m3, cylindrical compressive strength 8.5MPa and water absorption ratio 6% an hour as coarse aggregate and river sand. The concrete mix design was made based on the guidelines of the relevant Chinese standards. The adopted mix parameters are shown in Table 1. In order to ensure proper compaction, a high degree of workability i.e. 80–100 mm slump is adopted for the concrete mixes and is achieved by using silica fume and superplasticizer as admixtures. Three standard concrete cubes (150 mm size) and three prisms ([150x150x300] mm) were cast and warped in polyethylene sheets, then stored at room temperature, without wet curing to simulate conditions similar to that of concrete in the columns. The concrete cubes and prisms tested when the corresponding specimens tested to find out the concrete grade, compressive strength (f_{ck}) and Young's modulus (E_c) of the unconfined concrete at 28 days respectively.

Table 1: The Mix Component and Parameters

Component	Mix Parameters
Cement content	460 kg/m^3
Ceramisite	670 kg/m^3
Sand	650 kg/m^3
Water	150 kg/m^3
Silica fume	43kg/m^3
Super-plasticizer	3.8 kg/m^3
Concrete bulk density	1810 kg/m^3
Characteristic 28-days concrete cube strength	44.7 MPa
Characteristic 28-days concrete prism strength f_{ck}	35.2 MPa
the Young's Modulus of concrete E_c	26.2 GPa

The steel tubes were made up of mild steel plates, with yield strength (f_y) of (274.7) MPa and three different lengths (L= 342, 798 and 1596 mm). All tubes are seam welded and its edges are finished. After the fabricating of the steel tube, a 10 mm thick circular flat plate (with a diameter slightly larger than that of the steel tube) welded to its base to support the wet concrete during casting. The concrete was then vertically cast into the steel tube in about four equal layers, where each layer compacted by using a poker vibrator. Surface hollow due to concrete shrinkage was filled up with grout to confirm the specimen side smoothness and ensure both steel and concrete being loaded together. After 24–hours of treatment; another 10 mm thick circular plate was welded on the other side. Finally, the columns were stored at room temperature for 28 days.

According to reference [3], stub column defined as the one with $L/D \leq 3$ and medium length column is the one with $L/D > 3$ in this experiment. To study the mechanical properties of LACFT columns; specimens with two different t/D ratios (11% and 13.5%) three different L/D ratios (3, 7 and 14) were chosen in this test. The geometric and material properties of the specimens and the test results are summarized in Table 2.

2.2 Test Setup and Procedure

The tests are conducted on LACFTs, in a 3000 kN capacity column testing machine at 28 days of age. At the two ends of the specimen utilized column joint to simulate the hinged boundary conditions. For the safety and accuracy of the specimen tests, three round holes of 20 mm diameter and 15 mm depth were set according to the 10 mm, 20 mm, 35 mm eccentric distances far from the center of the bottom column roller. During the test a steel rabbet with a diameter of 20mm and 25mm length was used to connect specimen's plate with the column joint. For the deformation measurements, eight strain gauges were setup up at the mid-length of the column to record strains values. In the bending plane three displacements gauges were installed; the top and the bottom ones were at distance of one fourth the height of each column from the top and the bottom respectively and the third displacement gauge was positioned at the mid-height of each column to measure the lateral deformation. In order to measure the vertical deformation two displacements gauges were setup. All these gauges were connected to a computer data acquisition system to record their values in the whole test phases. Before the tests, a preload of about 2–5 kN was applied so the platens of the testing machine firmly attached to both ends of the specimen. The load applied at rate of 1/10 and 1/15 of the predicted ultimate load in the elastic phase and in the column yielding phase respectively. Every load preserved two to three minutes to enable the full deformation**.**

Table 2: Details of the test specimens

columns	**Size** $D\times t\times L$ (mm)	**eccentricity distances** e_0(mm)	t/D **(%)**	L/D	f_y (MPa)	f_{ck} (MPa)	**Mean Ultimate strength** N_u(kN)
A1-3-a,b,c	114×3×342	10	11.4	3	274.7	35.2	649.63
A2-3-a,b,c	114×3×342	20	11.4	3	274.7	35.2	531.73
A3-3-a,b,c	114×3×342	35	11.4	3	274.7	35.2	400.90
B1-3-a,b,c	114×3.5×342	10	13.5	3	274.7	35.2	706.30
B2-3-a,b,c	114×3.5×342	20	13.5	3	274.7	35.2	582.16
B3-3-a,b,c	114×3.5×342	35	13.5	3	274.7	35.2	423.56
A1-7-a,b,c	114×3×798	10	11.4	7	274.7	35.2	559.48
A2-7-a,b,c	114×3×798	20	11.4	7	274.7	35.2	428.81
A3-7-a,b,c	114×3×798	35	11.4	7	274.7	35.2	314.12
A1-14-a,b,c	114×3×1596	10	11.4	14	274.7	35.2	503.79
A2-14-a,b,c	114×3×1596	20	11.4	14	274.7	35.2	390.74
A3-14-a,b,c	114×3×1596	35	11.4	14	274.7	35.2	295.75
B1-7-a,b,c	114×3.5×798	10	13.5	7	274.7	35.2	591.83
B2-7-a,b,c	114×3.5×798	20	13.5	7	274.7	35.2	437.44
B3-7-a,b,c	114×3.5×798	35	13.5	7	274.7	35.2	354.45
B1-14-a,b,c	114×3.5×1596	10	13.5	14	274.7	35.2	524.34
B2-14-a,b,c	114×3.5×1596	20	13.5	14	274.7	35.2	434.43
B3-14-a,b,c	114×3.5×1596	35	13.5	14	274.7	35.2	330.65

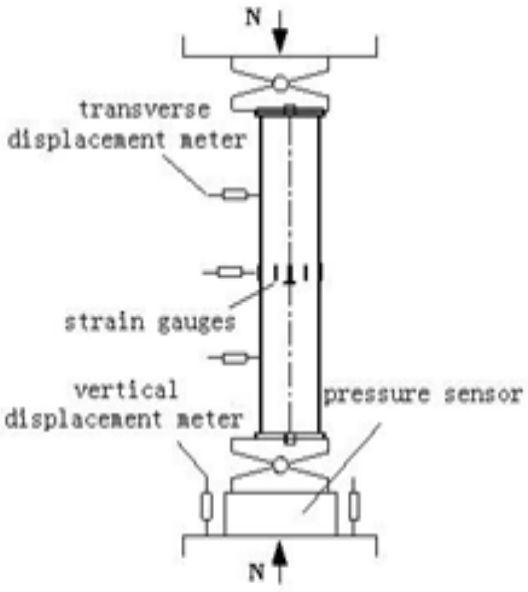

Figure 1: Loading and Measurement system

When approaching the ultimate load, slow loading mode was applied. Any one of these two conditions noticed conclude the test: (1) the maximum deformation reached, (2) or obvious features of failure occurred in the specimens.

3 Results and Discussion

3.1 The Test Phenomena and Failure Mode

Specimens have shown Different failure modes illustrated in figure 2. The Experimental characteristics were observed in the course of columns test: bow-shaped appeared on the surface of steel tube also the surface showed different degrees of drum bending. Besides, large lateral deflection with instability and unobvious circumferential deformation except the lateral one were also observed in the columns having L/D> 3. Figure 3 is a typical specimen's displacements distribution picture showing the lateral deflection degrees along the length of the component. From the figure, it can be seen that the deflection of specimens gradually increased with the load growing and the form of deflection curves accord with the sinusoidal half wave.

Figure 2: Typical failure modes of specimens

Strain distribution Curves of the specimens middle section for three different eccentric ratios are shown in figure 4, where "+" and "-" signs represents compressive and tensile strains respectively.

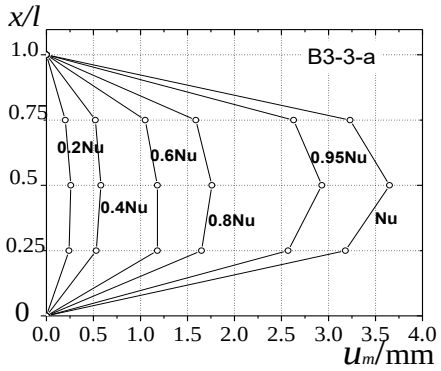

Figure 3: Deflection along the length measured with the displacement meters

From figure 4 it is observed, the section deformation of specimen's agree with the plane section assumption in each loading stage. Level of correspondence for plane section at initial loading stage was better than later loading stages. For small eccentric ratios, neutral axis location moved gradually to the load location along with load increasing, but it was unobvious for large eccentric ratios.

3.2 Analysis of Failure Course

The load–strain curves of LACFT are shown in figure 5. According to this figure, at elastic phase the curves (OA and O'A') of the columns with $L/D \le 3$ and $L/D > 3$ are similar and approximated linearly. It is clear that all the curves of various samples are almost coincidence at this phase. The proportional limit load (A and A') is 60% to 70% of the ultimate load. As the load increases, the curves gradually deviates from straight line and enters into the elastic-plastic stage (AB and A'B'), concurrently the compression zone of steel tube begins to yield, and the lateral deflection of all specimens became larger. At the ultimate load, the curves enters into the descending stage (BC and B'C'), where the bearing capacity decreased with the increment of the lateral deflection, and the curve declined more tardily. It is observed that the LACFT columns have been able to maintain greater capacity, and good ductility performance, simultaneous with various degrees of partial bending drum appeared on the surface of the steel tube; hence filled with lightweight aggregate concrete can effectively delay the deflection of steel tube. The curves of columns ($L/D > 3$) have showed that the larger eccentricity ratio is the larger longitudinal strain would be. Therefore large overall deformation and lateral buckling were occurred in specimens.

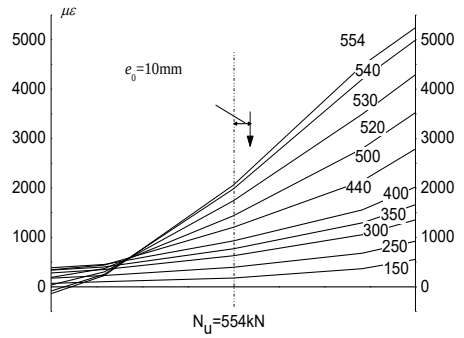

(a) A1-7-a

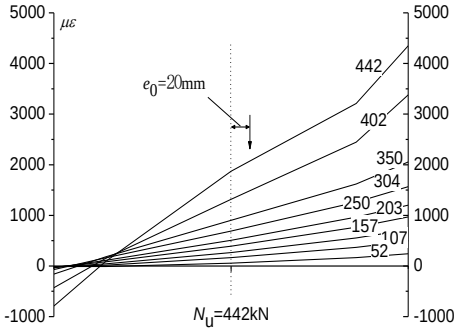

(b) A2-7-a

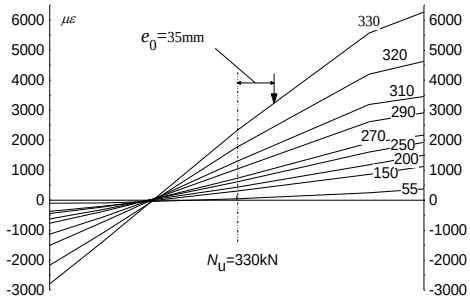

(c) A3-7-a

Figure 4 (a), (b) and (c): Curves of strain distribution for different eccentric ratios

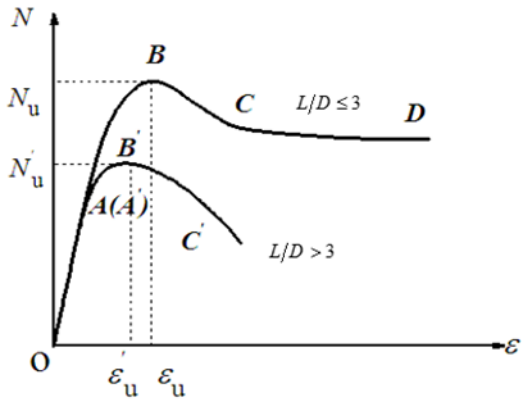

Figure 5: Sketch map of $N-\varepsilon$ curves

3.3 Analysis of Failure Mechanism

Figure 6 illustrates Poisson's ratio (ν) of the composite materials versus bearing capacity in different regions of the cross-section. This ratio is usually 0.25 to 0.3, and the average one is 0.283. However, as Poisson's ratio of the concrete is lower than that of steel; steel tube breeds a constraint effect on the concrete [6]. From figure 6, in the initial stage of loading, Poisson's ratio in the regional cross-section of steel tube mainly maintain about 0.2 to 0.3, therefore, the constraint effect of steel tube on the concrete is smaller. In the elastic-plastic phase, at the edge of the compression zone the Poisson's ratio significantly increased close to the ultimate load, at the same time gradual increase occurred at the symmetry axis, but at the edge of the tension section the ratio preserve unchanged or with a little change. Hence circular steel tubes under eccentric load are able to generate the constraint effect on the core concrete. Also, it was noticed, the larger Poisson's ratio of the steel tube is the stronger confinement effect on the LAC core.

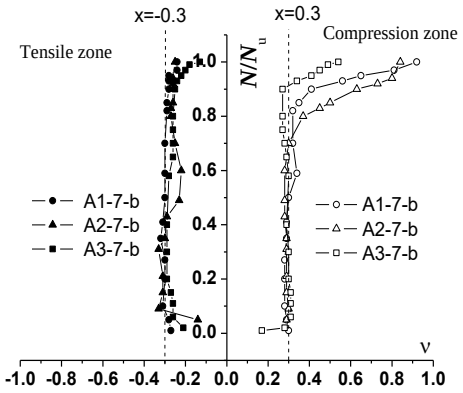

Figure 6: N/N_u versus Poisson's ratio (ν) of the composite material in the cross-section of mid-span

4 The Influencing Parameters of the Columns

4.1 Influence of Eccentricity Ratio

To analyze the relation of eccentricity ratio versus bearing capacity of the columns under eccentric axial compression load, stress-strain curves of different specimens which have similar steel and concrete characteristic properties but with various eccentric ratios were visualized in figures 7 (a) and (b). These figures have shown that as a result of the influence of large eccentricity; the bearing capacity and rigidity decreased, while the ductility performance effectively improved. As a conclusion could be argued that; the greater the eccentricity ratio, the less the ultimate bearing capacity, therefore the constraint effects in this case has less impact on the improvement of bearing capacity of the LACFT columns.

4.2 Influence of Thickness to Width ratio

In the early stage of loading and by using different t/D ratios, the load versus deformation curves in the middle of columns have shown almost similar slope (figure 8 (a)). But in a later stage of loading, these curves showed a clear separation (figure 8 (b)). Thus; as the t/D increases, the slopes of the curves increase, as well as the ultimate bearing capacity of the columns. This behavior certify the growth of the confinement effect achieved by increasing t/D ratio on LAC core, has improved specimen's strength by developing extra moment of resistance in the compression zone, with the progress of Poisson's ratio.

4.3 Influence of Length to Width Ratio

Figure 9 shows the influence of length to width ratio on the columns with $L/D > 3$. At the initial loading stage, specimen's materials have displayed elastic behavior concurrent with small lateral deformation, and small additional moment caused by the lateral deformation under eccentric load. In elastic-plastic stage additional moment occurred, due to the growing of the specimen's longitudinal deformation as a result of L/D ratio increasing, hence, smaller ascending slope and lower bearing capacity were achieved.

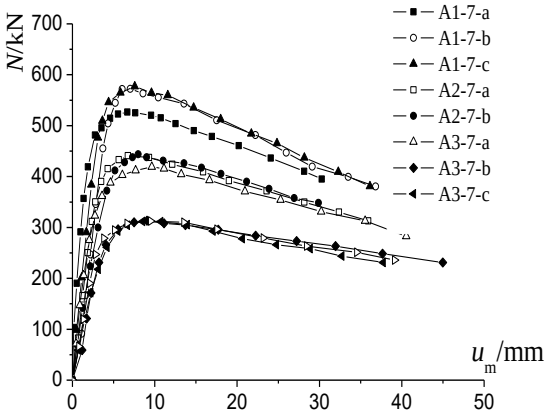

(a)

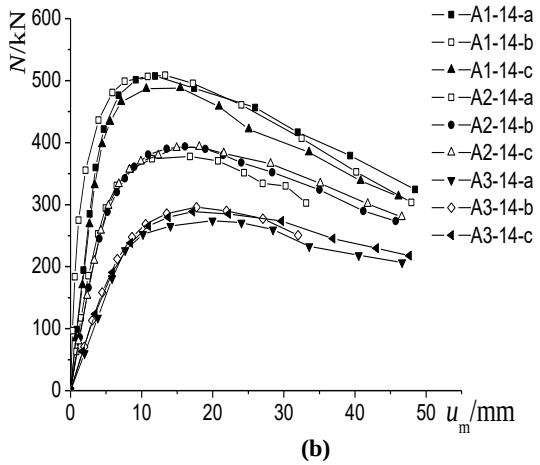

(b)

Figure 7 (a) and (b): N- ε for different eccentricity ratios

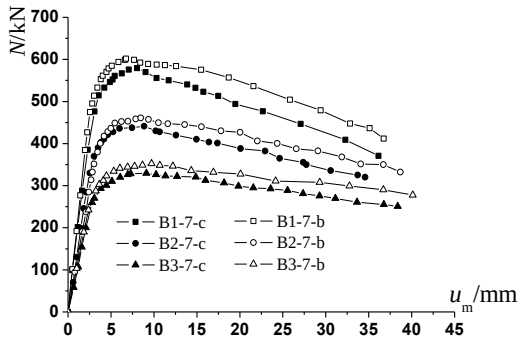

(a)

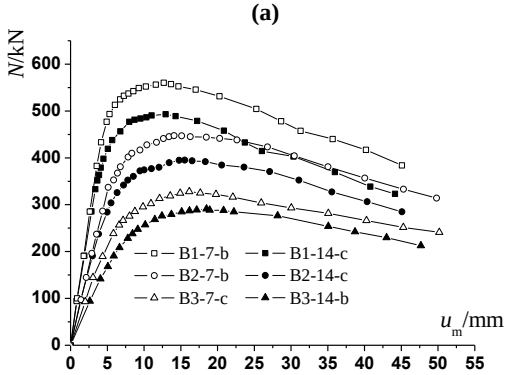

(b)

Figure 8 (a) and (b): N-u_m for different t/D ratios

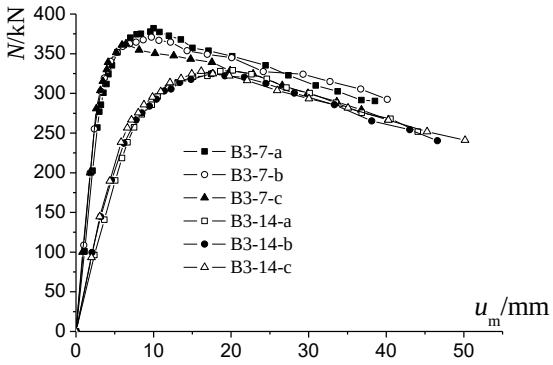

Figure 9: N-u_m for different L/D ratios

5 Comparison and Analysis of Ultimate Bearing Capacity of Columns

The feasibility of currently available design codes in predicting the bearing capacity of LACFT columns subjected to eccentric compression load, evaluated by comparing the calculated values according to the references 7, 8 and 9 with the ones gained from experiment. Table 3 shows, the calculated bearing capacities of LACFT columns which calculated according to the references 7, 8 and 9 are underestimated, applicable and have a good agreement in compare with the test results ones respectively. Therefore it is possible to say the formulas of the references: 7, 8 and 9 capable to estimate the bearing capacity of the LACFTs columns.

Table 3: N/Nu for different code provisions

Columns	Test mean	AISC-LRFD 1999		DBJ13-51 2003		CECS 28:90 1990	
	N_u(kN)	N(kN)	N/N_u	N(kN)	N/N_u	N(kN)	N/N_u
A1-3-a,b,c	649.63	306.16	0.471	522.47	0.804	628.23	0.967
A2-3-a,b,c	531.73	232.51	0.437	421.09	0.792	500.06	0.94
A3-3-a,b,c	400.90	170.86	0.426	326.03	0.814	383.69	0.957
B1-3-a,b,c	706.30	326.23	0.476	563.97	0.797	687.06	0.973
B2-3-a,b,c	582.16	258.47	0.444	452.87	0.778	546.51	0.939
B3-3-a,b,c	423.56	191.90	0.453	350.23	0.827	417.05	0.985
A1-7-a,b,c	559.48	304.04	0.543	464.97	0.831	502.80	0.899
A2-7-a,b,c	428.81	231.30	0.539	370.50	0.864	400.58	0.934
A3-7-a,b,c	314.12	170.21	0.542	284.38	0.905	306.98	0.977
B1-7-a,b,c	591.83	296.36	0.501	382.26	0.646	399.53	0.675
B2-7-a,b,c	437.44	226.82	0.519	302.66	0.692	318.30	0.728
B3-7-a,b,c	354.45	167.77	0.473	231.75	0.654	243.92	0.688
A1-14-a,b,c	503.79	333.62	0.662	504.99	1.002	550.14	1.092
A2-14-a,b,c	390.74	256.93	0.658	402.96	1.031	437.68	1.120
A3-14-a,b,c	295.75	191.06	0.646	309.69	1.047	334.97	1.133
B1-14-a,b,c	524.34	324.18	0.618	418.85	0.799	437.16	0.834
B2-14-a,b,c	434.43	251.29	0.578	333.07	0.767	347.79	0.801
B3-14-a,b,c	330.65	187.92	0.568	256.10	0.774	266.17	0.805
Average			0.531		0.824		0.914
S.D			0.078		0.114		0.136

6 Conclusions

The following observations and conclusions are made based on the limited test results described in this paper are:

1. The greater the eccentricity ratio, the less the ultimate bearing capacity, therefore the influence of large eccentricity; the bearing capacity and rigidity decreased, while the ductility performance effectively improved.
2. The greater the thickness to width ratio, the greater the ascending slope of the curves, as well as increased the ultimate bearing capacity.
3. Length to width ratio has great effect on the columns with but has no or has negligible effect on the columns with. Moreover, load versus deformation curves by different L/D ratio have smaller ascending slope hence lower bearing capacity achieved.
4. Comparisons are made with the predicted column strength using the existing codes such as AISC-LRFD (1999), CHN DBJ 13-51-2003 (2003) and CHN CECS 28:90, the calculated bearing capacities of LACFT by AISC-LRFD are underestimated in compare to that of the test results due to the neglect of steel tube confinement effect, while the calculated value of CHN DBJ 13-51-2003 (2003) are applicable with slightly overestimated values for L/D ≥ 14, but the values predicted by CHN CECS 28:90 have a good agreement with the experimental results with slightly overestimated values for L/D ≥ 14 too.
5. In present it has not yet been lunched a calculation formula for the LACFT bearing capacity; therefore the formulas of the references (AISC-LRFD 1999), (DBJ13-51 2003) and (CECS 28:90 1990) can be adopted to estimate the eccentricity bearing capacity of the LACFT columns.
6. More experimental investigations are needed to setup new formulas which are able to figure out the problem of the design of composite columns fabricated from lightweight aggregate concrete filled in steel tube.

References

[1] Shams M, Saadeghvaziri MA. State of the art of concrete-filled steel tubular columns, ACI Struct J, 94(5), 558–71, 1997.

[2] Liu Dalin, Gho Wie-Min, Yuan Jie. Ultimate capacity of high-strength rectangular concrete-filled steel hollow section stub columns, J Constr Steel Res, 59:1499–515, 2003.

[3] Ji Bohai, Yang Ming, Chen Jiashu, Confinement effect and strength criterion of lightweight aggregate concrete confined by steel tube, Bridge Constr., (4), 11－14, (2006).

[4] Zuobin Wei, XiliangLiu, The fundamental function studies of steel tube cover hoop ceramicist concrete, Proceedings of '93 China Steel's, steel - concrete composite structure Association 4th Annual Meeting, Guangzhou, (1993).

[5] M. Mouli, H. Khelafi, Strength of short composite rectangular hollow section columns filled with lightweight aggregate concrete, J. Eng. Struct., (29), 1791-1797, 2007.

[6] Han linhai and Yang youfu, Modern Concrete filled steel tubular structures, 1st edition, China building industry Press, Beijing China, 2004. (In Chinese)

[7] AISC-LRFD (1999), American Institute of Steel Construction, "Load and Resistance Factor Design Specification for Structural Steel Buildings Chicago (IL)".

[8] DBJ13-51-2003 (2003), Fuzhou University, "Technical Specification for Concrete-Filled Steel Tubular Structures", Fujian Province. (In Chinese)

[9] CECS 28:90 (1990), Construction Standard Committee of China, "Chinese Specification for the Design and Construction of Concrete-Filled Steel Tubular Structures", Planning Publishing House of China Beijing. (In Chinese)